

## Supplementary Materials for **Synchronous Change of Atmospheric CO<sub>2</sub> and Antarctic Temperature During the Last Deglacial Warming**

F. Parrenin,\* V. Masson-Delmotte, P. Köhler, D. Raynaud, D. Paillard, J. Schwander, C. Barbante, A. Landais, A. Wegner, J. Jouzel

\*Corresponding author. E-mail: parrenin@ujf-grenoble.fr

Published 1 March 2013, *Science* **339**, 1060 (2013)  
DOI: 10.1126/science.1226368

**This PDF file includes:**

Materials and Methods  
Supplementary Text  
Figs. S1 to S8  
Tables S1 to S7  
References

**Other Supplementary Material for this manuscript includes the following:**  
(available at [www.sciencemag.org/cgi/content/full/339/6123/1060/DC1](http://www.sciencemag.org/cgi/content/full/339/6123/1060/DC1))

Database S1

## Materials and Methods

### Estimating Δdepth from air $\delta^{15}\text{N}$ data

The principles of using air  $\delta^{15}\text{N}$  data to estimate  $\Delta\text{depth}$  have been described elsewhere (1). It is not possible to directly use the raw  $\delta^{15}\text{N}$ -based  $\Delta\text{depth}$  estimates because they are noisy. As a proof, the  $\partial\Delta\text{depth}/\partial z$  function estimated from these raw data (1) sometimes exceeds 1, which would mean that the gas layers are inverted. The reason is probably the ice quality, since 1) the ice is brittle at these depths; 2) the pooled standard deviation of the measurements is only  $<0.012\text{\textperthousand}$  (2), equivalent to  $\sim 2$  m of LID and is not significantly higher for the last deglaciation than for older time periods. We therefore apply a 13 points moving average fit (Fig. 1). The fit is extrapolated in the 340-376.35 m and 561.31-600 m intervals by assuming the LID in ice equivalent is constant and only the variations of ice thinning impact  $\Delta\text{depth}$ . We inferred that 13 was the optimal number of points for the running average by studying the residuals: using less points results in anti-correlated residuals while using more points results in correlated residuals. By doing this smoothing, we assume that on average, the  $\delta^{15}\text{N}$  data are representative of the  $\delta^{15}\text{N}$  content of the air at the bottom of the diffusive zone. This is corroborated by the quasi-symmetrical distribution of the residuals (2). Based on the standard deviation of the distance of the  $\delta^{15}\text{N}$ -based  $\Delta\text{depth}$  estimates to the fit (linearly interpolated in depths), we estimate their  $1\sigma$  accuracy to be  $\sim 2$  m, which translates into a 0.6 m  $1\sigma$  accuracy for the fit. We neglect the error in the linear interpolation in depths procedure because the average sampling is only  $\sim 2.4$  m. We also added  $1\sigma$  uncertainties of 1% due to the dependence of the gravitational enrichment to the poorly known temperature during the past (1), 0.5% due to the poorly known temperature gradient in the firn (1) and 2.5% due to the poorly known average firn relative density (1). Another source of uncertainty is due to the thinning function evaluation. It has been evaluated to range between 1% and 1.8% in the 340-600 m depth interval considered here (1).

In our study we have assumed that the past convective zone thickness was negligible. One potential cause for variations in this physical variable is the change in surface winds. GCM experiments for the LGM shows little variations in wind on the East Antarctic plateau (3).

### Construction of the age scale

Our ice age scale is a modified version of the EDC3 ice age scale (4). We first corrected for a depth offset between the EDC96 and EDC99 ice cores and added 55 yr to the EDC3 age scale for ages older than 45.6 kyr. We then computed gas ages from this EDC3<sub>corr</sub> ice age scale for the EDC CH<sub>4</sub> record (5) based on our  $\delta^{15}\text{N}$ -based  $\Delta\text{depth}$  estimates. We found that this new gas age scale does not perfectly fit with the GICC05 age scale (6) by comparing the CH<sub>4</sub> transitions (7). We therefore decided to modify the EDC3<sub>corr</sub> ice age scale in the interval between 5280 yr b1950 (where there exists an absolute tie point derived from the comparison between Antarctic <sup>10</sup>Be and <sup>14</sup>C from the dendrochronology)

and 41,200 yr b1950 ( $^{10}\text{Be}$  peak corresponding to the Laschamp geomagnetic event). We therefore linearly interpolated the EDC3<sub>corr</sub> ice age scale according to the tie points listed in Table S1 to get a perfect fit with ages ties (see 3 for the resulting CH<sub>4</sub> synchronization to GRIP/GICC05). This ice age scale has however negligible impact on the discussion of the aCO<sub>2</sub>-AT phasing, which mainly depends on the  $\Delta$ depth estimates.

### An Antarctic temperature stack, 0-800 kyr b1950

Here we produce a stack of Antarctic temperature variations during the past 800 kyr, based on available ice core data (Table 2) at EPICA Dome C (EDC), Dome Fuji (DF), Vostok, Talos Dome (TALDICE) and EPICA Dronning Maud land (EDML). A preliminary work is the synchronization of all the DF, Vostok, TALDICE and EDML ice cores to the EDC one, based on volcanic matching, where available and isotopic matching elsewhere (using the break points). The isotopic records at each site are converted to temperature records using the classical isotopic thermometer, with correction for  $\delta^{18}\text{O}$  variations in the ocean caused by land ice variations. The stack is then simply constructed, for each time in the past, as the average of all available ice core temperature records.

Ice isotope variations recorded in ice cores are corrected for ocean sea water (SW) isotope variations following the approach by Stenni et al. (8):

$$\delta^{18}\text{O}_{corr} = \delta^{18}\text{O}_{ice} - \delta^{18}\text{O}_{sw} \times \frac{1 + \delta^{18}\text{O}_{ice}/1000}{1 + \delta^{18}\text{O}_{sw}/1000} \quad (1)$$

$$\delta D_{corr} = \delta D_{ice} - 8 \delta^{18}\text{O}_{sw} \times \frac{1 + \delta D_{ice}/1000}{1 + 8 \delta^{18}\text{O}_{sw}/1000} \quad (2)$$

$\delta^{18}\text{O}_{sw}$  has been inferred (9) based on an ocean isotopic stack (10). We put the  $\delta^{18}\text{O}_{sw}$  record on the EDC3 age scale by synchronizing the polar temperature reconstruction (9) with the EDC isotopic record (see Table 6).

The temperature at each ice core site is then simply evaluated as:

$$\Delta T_{clim} = 1/\alpha \times \Delta \delta D_{corr} \quad (3)$$

or

$$\Delta T_{clim} = 8/\alpha \times \Delta \delta^{18}\text{O}_{corr} \quad (4)$$

with  $\alpha=6.04\text{‰}/^{\circ}\text{C}$  (11). First, we shift the EDC temperature reconstruction to obtain an average  $\Delta T_{clim}=0$  over the time interval 0-1 kyr b1950. Second, we rescaled the temperature reconstruction from each ice core so that the resulting  $\Delta T_{clim}$  has the same average and standard deviation than the EDC one on the interval 0-140 kyr b1950, where all ice cores temperature reconstructions are available.

The EDC3 chronology (4) is transferred onto each ice cores using the tie points described above. Each temperature record is then resampled using an averaging over 20 yr intervals. For each of these 20 yr long time interval, the average of all available ice core temperature reconstructions is computed. The stack is again further scaled to have a 0

average over the time interval 0-1 kyr b1950. A pooled standard deviation is calculated for the stack, as:

$$\sigma_{\text{pooled}} = \sqrt{\frac{\sum_{i,j=1}^{n,m} (T_i - \bar{T}_j)^2}{n-m}}, \quad (5)$$

which is the root of the sum of the squared differences of the individual temperature reconstructions  $T_i$  from the stack  $\bar{T}_j$  divided by the degree of freedom, in this case the number of individual temperature values  $n$  minus the number of stacked temperature values  $m$ . For each age, the confidence interval of the stack is simply evaluated as:

$$\sigma = \frac{\sigma_{\text{pooled}}}{\sqrt{N}}, \quad (6)$$

where  $N$  is the number of available isotopic records.

#### Fit of AT, aCO<sub>2</sub> and rCO<sub>2</sub> by 6 points linear functions

We search for the 6 points continuous and linear by interval functions (Figure S5) which best fit the AT, aCO<sub>2</sub> and rCO<sub>2</sub> records defined by  $N$  data points  $(t_i, y_i)$ . We define the density of probability of such a fit  $y(t)$  defined by its 6 points  $(T_i, Y_i)$ ,  $i=0, \dots, 5$  (we fix  $T_0=9000$  yr and  $T_5=22000$  yr the boundaries of our time interval), by:

$$P = k \cdot \exp \left( -\sum_{i=0}^N \frac{(y(t_i) - y_i)^2}{\sigma^2} \right), \quad (7)$$

where  $k$  is a multiplicative constant,  $\sigma$  is an uncertainty which includes both the uncertainty on the data value  $y_i$  and the uncertainty of the 6 points linear model (12). In practice,  $\sigma$  is evaluated as the standard deviation of the residuals of the data value  $y_i$  to a first best 6 points linear function (Figure 6). By writing Equation (7), we implicitly assume that those uncertainties for each data point  $y_i$  are independent. In such a case, the modeling uncertainties are correlated at short time scales. Again by studying the residuals (Figure 6), we evaluated that there is no correlation for a distance between the  $t_i \geq 200$  yr for AT and  $\geq 400$  yr for aCO<sub>2</sub> and rCO<sub>2</sub>. We thus resampled the AT, aCO<sub>2</sub> and rCO<sub>2</sub> records every 200 yr, 400 yr and 400 yr respectively. The evaluation of  $\sigma$  is consequently updated to 0.177 °C for AT, 1.22 ppmv for aCO<sub>2</sub> and 0.0333 W/m<sup>2</sup> for rCO<sub>2</sub>. Our resampling approach is conservative and probably overestimates the real confidence intervals.

The densities of probabilities of  $T_i$ ,  $i=1, \dots, 4$  and  $Y_i$ ,  $i=0, \dots, 5$  are reconstructed by a Monte Carlo exploration based on the Metropolis-Hastings algorithm (13, 14). Note that the algorithm only needs to evaluate the ratio of the densities of probability between two scenario, thus there is no need to know the multiplicative constant  $k$ . The Monte-Carlo sampling is composed of 10,000 scenarii, which ensure robust statistics. We use here the mean and the standard deviation of the probability distributions. The inferred values for  $T_i$ ,  $i=1, \dots, 4$  and their confidence intervals are given in 7.

## Supplementary Text

### Discussion of the ATS stack

There are three main sources of uncertainties on estimates of past AT changes based on water stable isotopes from deep ice cores:

- Changes in elevation at the coring site (mainly due to accumulation variations and isostasy (15)) which can produce glaciological artefacts. While attempts have been conducted to correct for elevation changes using glaciological models (15-17), significant uncertainties remain (18).

- In the cases of Vostok and EDML, upstream effects induced by ice flow such as elevation variations, which are not corrected for in this study (18). These effects should be limited for TI.

- Changes in precipitation intermittency (and covariance between temperature and precipitation, at synoptic or seasonal scales). There is no mean to quantify such bias based on ice core data. While such bias has been simulated for climate projections (19) and suggested at the orbital scale (20), several climate model simulations suggest that this bias may be limited for central Antarctica, between LGM and present day (8, 16).

- Changes in moisture sources / evaporation conditions, affecting the initial water vapor isotopic composition. Information on past evaporation conditions (surface temperature, relative humidity) can be derived from deuterium excess and  $^{17}\text{O}$ -excess. The combination of such data and isotopic distillation models allows to quantify the impact of changes in moisture sources on reconstructed Antarctic temperature. Deuterium excess studies are available for Vostok (21), EDC and EDML (8, 22) and Dome F (23, 24).

Multiple ice core  $^{17}\text{O}$ -excess studies have recently been published (25). Despite significant methodological uncertainties (24), these studies suggest limited moisture source impacts on temperature reconstructions for the last deglaciation.

The oceanic correction applied to our isotopic records contains only long-term fluctuations (typical period is 20 kyr, the precession period) and therefore is thought to not impact the detection of the break points in AT.

Here we did not use the Byrd, Siple Dome and Law Dome ice cores because their isotopic records do not resemble the common central East Antarctic scenario, and thus could be affected by local biases (such as larger changes of ice sheet elevation (26)). For example, the Byrd isotopic record shows an early warming at the onset of TI which is not in phase with the onset of TI in other Antarctic ice cores (a fluorine spike can be used to assess such phasing). The Siple Dome isotopic record shows a sharp isotopic event at ~22 kyr b1950 which has no counterpart in other ice cores. The Law Dome isotopic record does not show a stable temperature scenario during the early Holocene (27) which makes the estimate of the youngest break point very uncertain.

Moreover, we did not use methane synchronization in our stack because 1) it is only robust when methane varies abruptly and this is for example not the case at the onset of TI

and 2) it requires to estimate the past LID from firn densification models and even for high accumulation sites like EDML and TALDICE, these models could for some periods overestimate the LID by ~20% (28), leading to an ice age scale ~300 yr too old.

An alternative isotopic stack has already been constructed for TI (29), using the records from Law Dome, Byrd, Siple Dome, EDML and TALDICE and based on methane synchronization. For the above mentioned reasons, we used here a different approach both for the synchronization of the ice cores and for the evaluation of the ice/gas shift. Both stacks are compared in Figure S4. The stack from (29) seems to be generally shifted by ~300 yr toward older ages with respect to our stack in the period from the onset of TI to the Antarctic Cold Reversal. This shift could be explained by either an overestimation of the modeled  $\Delta$ age or by local artefacts in the isotopic records of (29, 30), or by an underestimation of the convective zone thickness in our study, or by a combination of both.

#### **Additional Data file S1 (separate file)**

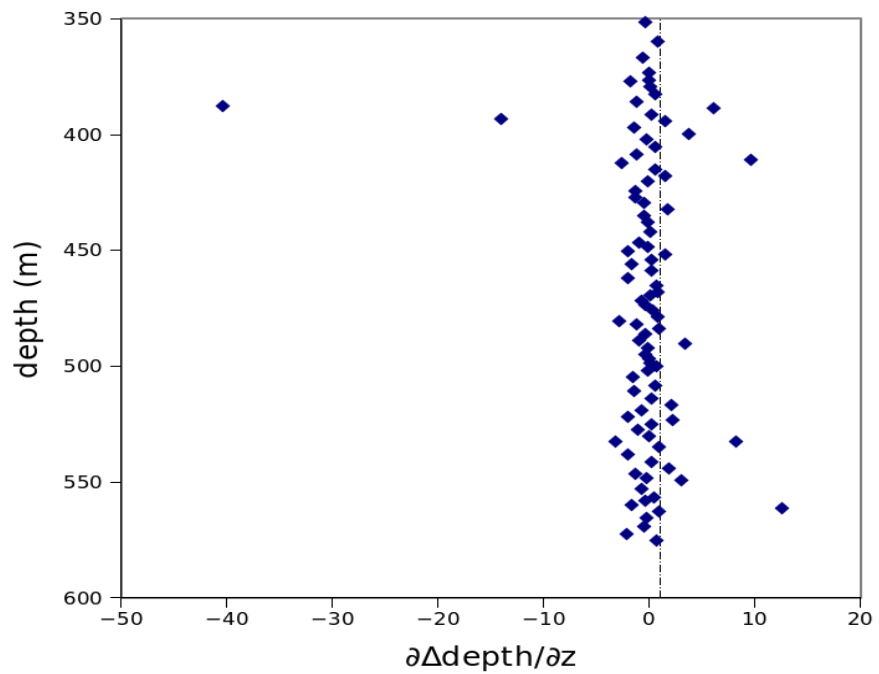


**Fig. S1**

$\partial\Delta\text{depth}/\partial z$  function as derived from the raw  $\delta^{15}\text{N}$ -based  $\Delta\text{depth}$  estimates. Vertical dashed line is for  $\partial\Delta\text{depth}/\partial z=1$ .

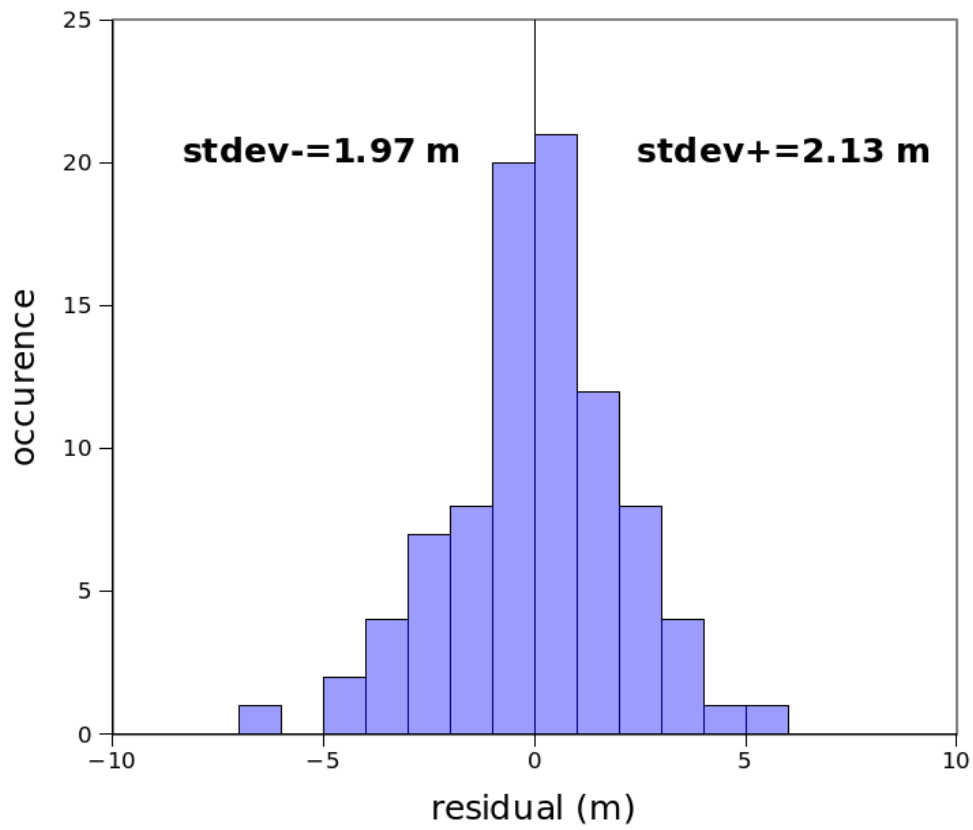


**Fig. S2**

Distribution of the residuals of  $\delta^{15}\text{N}$ -based  $\Delta$ depth estimates to the fit. The standard deviation to zero of the positive and negative residuals is indicated.

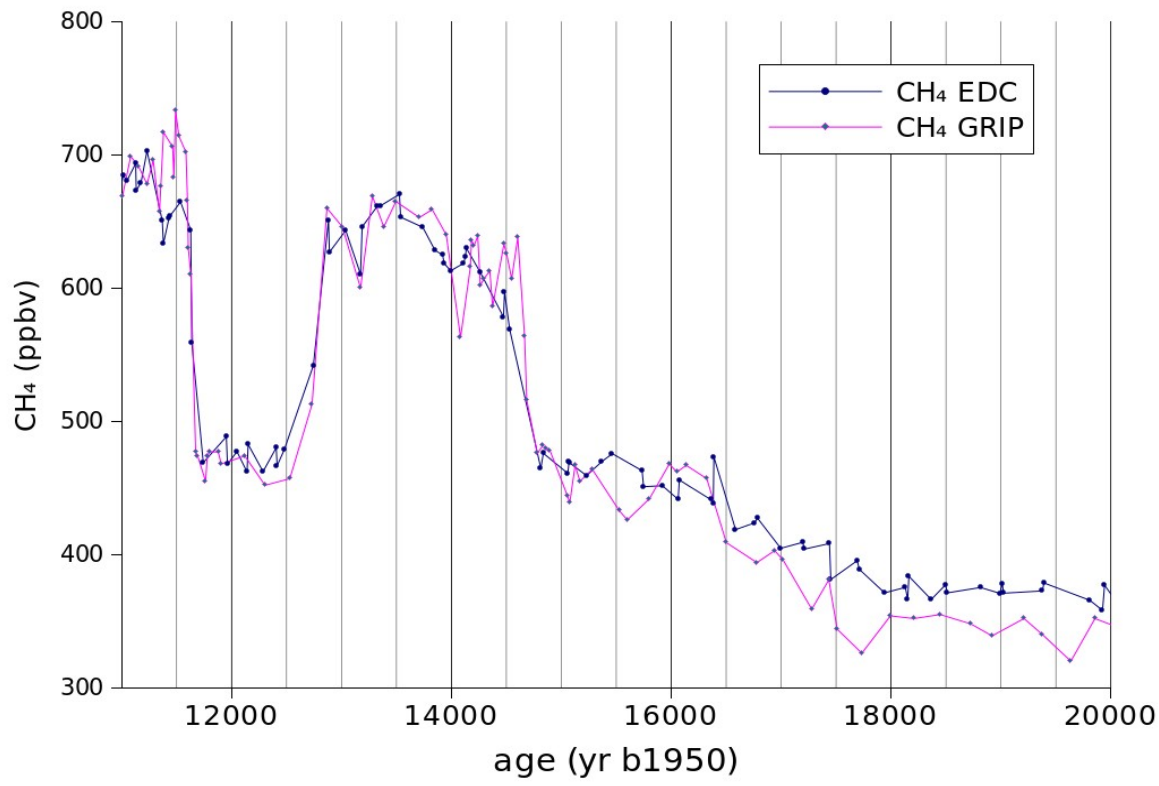


**Fig. S3**

Comparison between GRIP CH<sub>4</sub> record on the GICC05 age scale (7) with the EDC CH<sub>4</sub> record (5) on our age scale. GRIP CH<sub>4</sub> record is offset by -20 ppbv to take into account the interhemispheric CH<sub>4</sub> gradient during the 16-11 ka time interval.

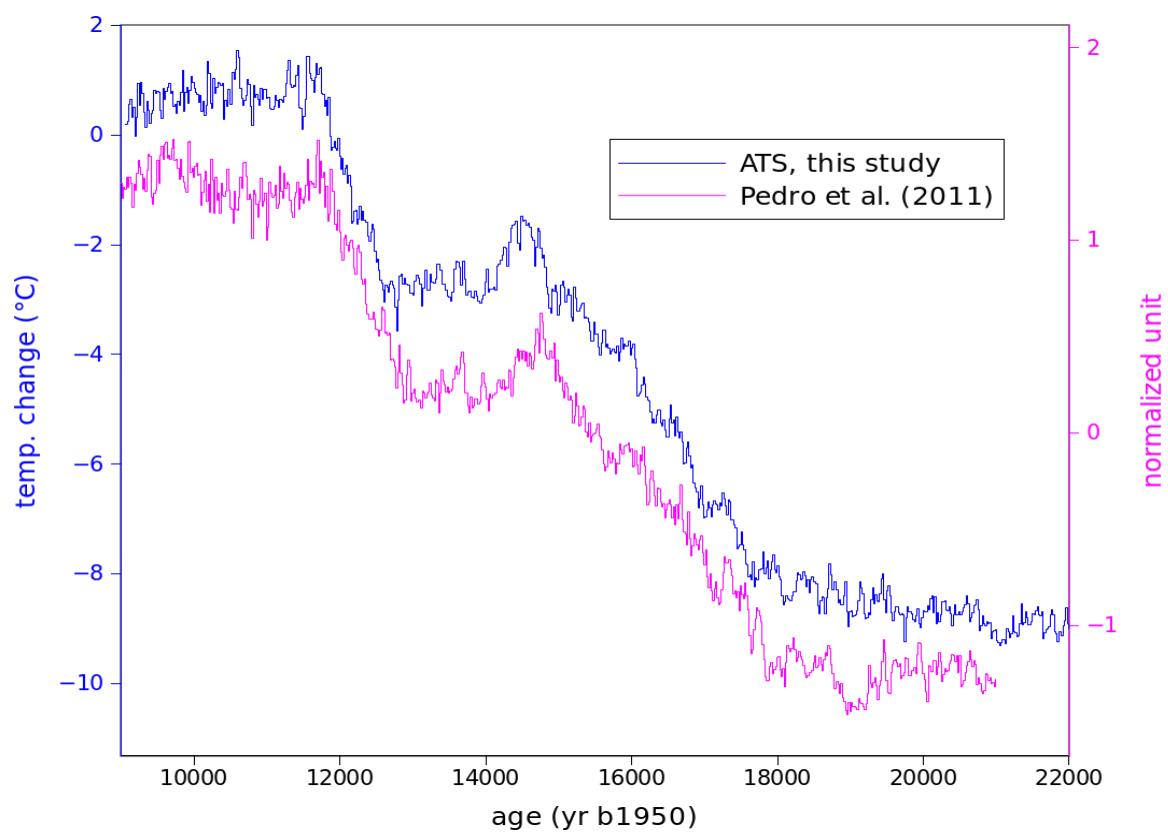


**Fig. S4**

Comparison of the ATS stack from this study with the Antarctic isotopic stack from (29).

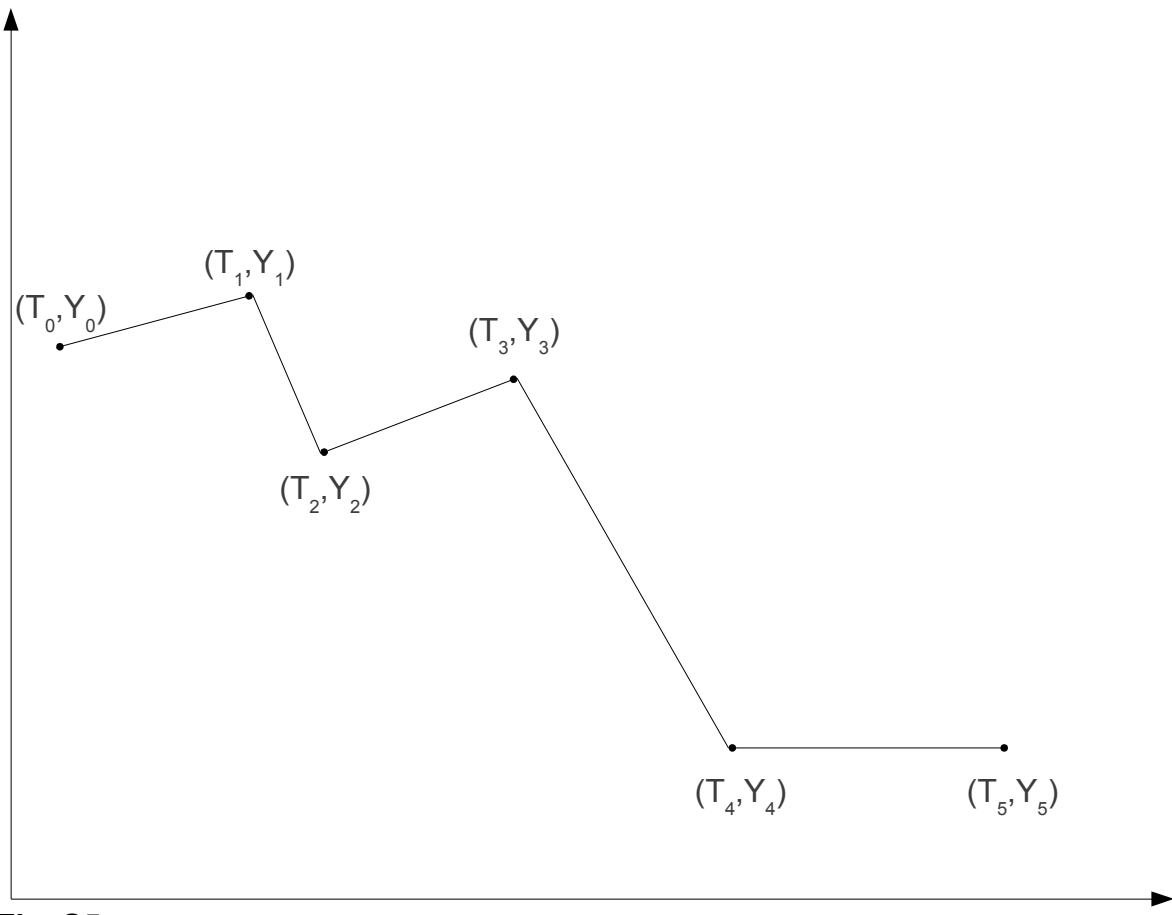


**Fig. S5**

Scheme illustrating a 6 points continuous and linear by interval function.

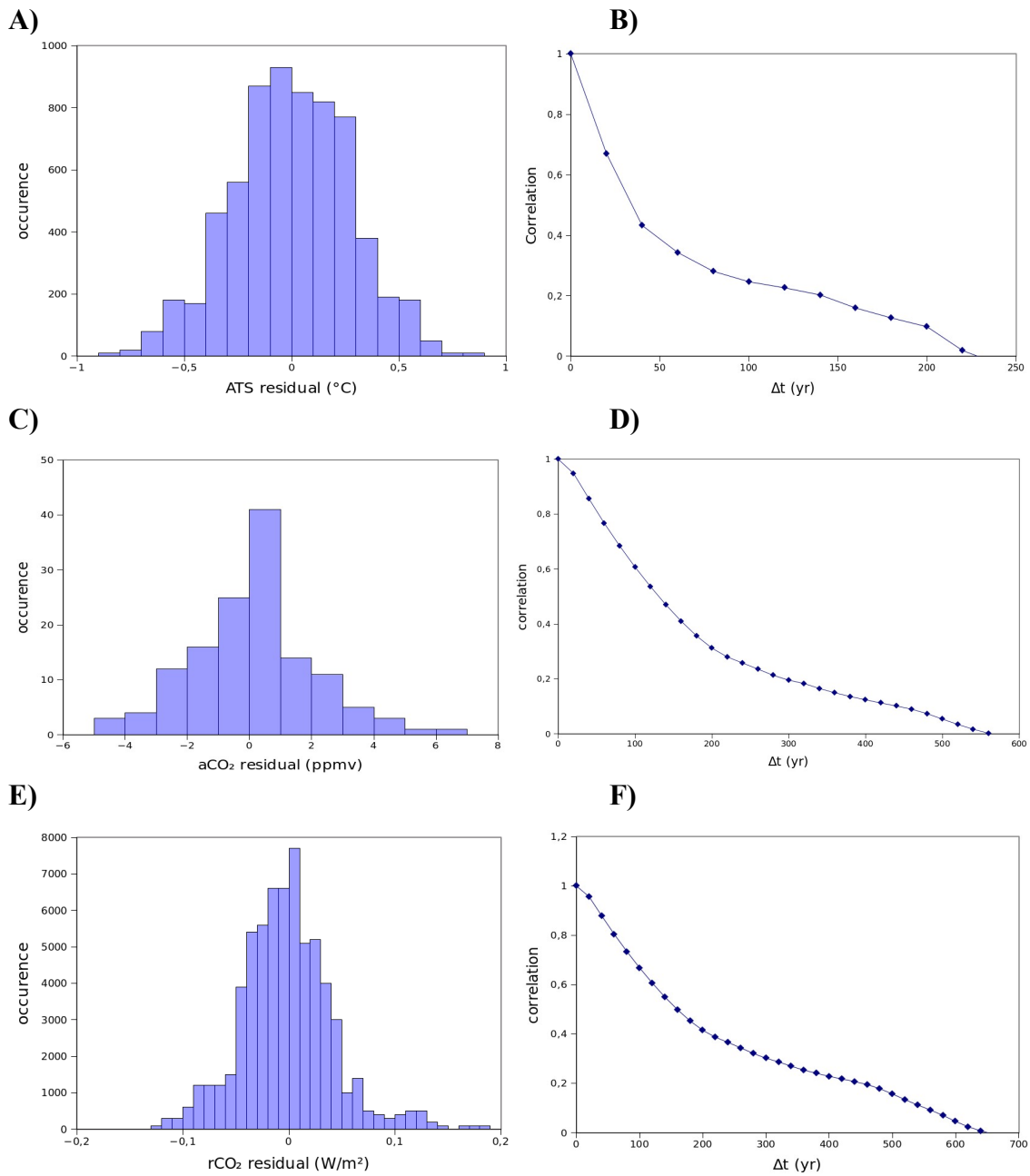


**Fig. S6**

Statistics on the residuals of the first best 6 points linear fit functions. **A)** Distribution of the AT residuals.  $\sigma=0.24^{\circ}\text{C}$ . **B)** Correlation of the AT residuals as a function of the time distance. **C)** Distribution of the aCO<sub>2</sub> residuals.  $\sigma=1.94 \text{ ppmv}$ . **D)** Correlation of the aCO<sub>2</sub> residuals as a function of the time distance. **E)** Distribution of the rCO<sub>2</sub> residuals.  $\sigma=0.049 \text{ W/m}^2$ . **F)** Correlation of the rCO<sub>2</sub> residuals as a function of the time distance.

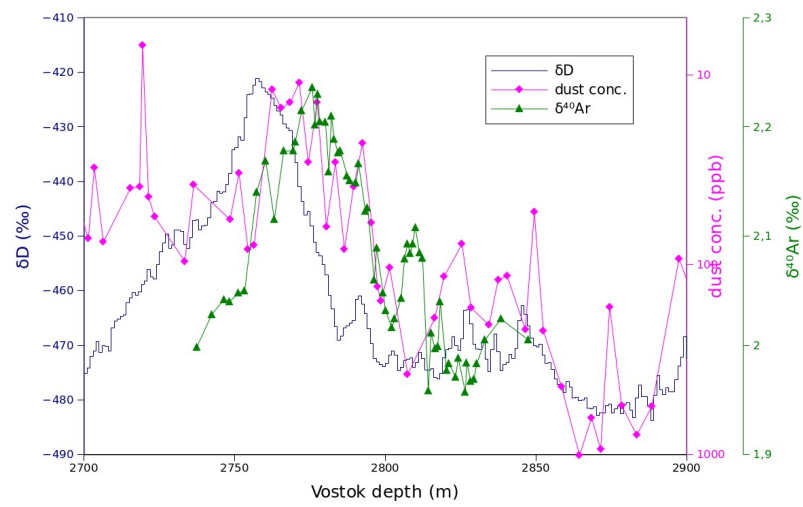


**Fig. S7**

$\delta D$  (31), dust concentration (31) and  $\delta^{40}\text{Ar}$  (32) records of TIII in the Vostok ice core.

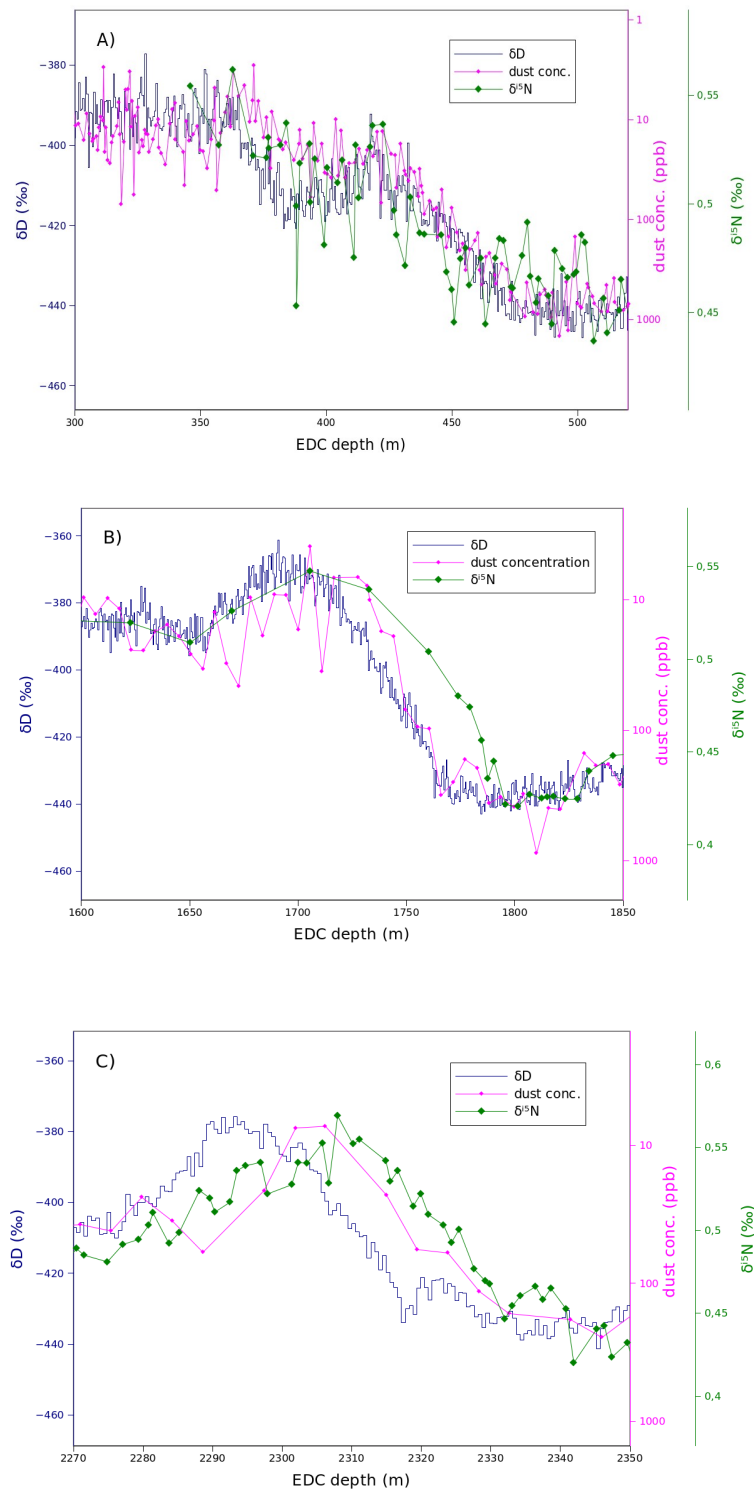


**Fig. S8**

$\delta D$  (16), dust concentration (33) and  $\delta^{15}\text{N}$  (2) records of TI (A), TII (B) and TIII (C) in the EDC ice core.

Tie points	EDC3 age (yr b1950)	Age this study (yr b1950)
<sup>10</sup> Be/ <sup>14</sup> C synchro	5280	5280
Onset of Holocene	11510	11600
Onset of Younger-Dryas	12810	12810
Onset of Bølling	14400	14680
Laschamp event	41200	41200

**Table S1**

Tie points between the EDC3 ice age scale and the ice age scale used in this study.

<b>Ice core</b>	<b>δD or δ<sup>18</sup>O</b>	<b>Extension</b>	<b>References</b>	<b>Synchronization to EDC</b>
EDC96	δD	0-45 kyr b1950	(16)	
EDC99	δD	45-800 kyr b1950	(16)	
DF	δ <sup>18</sup> O	0-335 kyr b1950	(34)	Table S3
Vostok	δD	0-415 kyr b1950	(31)	Table S4
TALDICE	δD	0-247 kyr b1950	(35)	(35) + Table S5
EDML	δD	0-140 kyr b1950	(36)	(37)

**Table S2**

Ice cores data used the construct the ATS stack.

Type	DF1 depth (m)	EDC99 depth (m)
surface	0	0
isotopic	356	360
isotopic	383	385
isotopic	419	419
isotopic	482	472
isotopic	610	585
isotopic	655	623
isotopic	671	635
isotopic	688	650
isotopic	745	700
isotopic	775	728
isotopic	792	740
isotopic	812	760
isotopic	854	800
isotopic	940	878
isotopic	966	900
isotopic	993	924
isotopic	1074	995
isotopic	1147	1062
isotopic	1188	1100
isotopic	1291	1200
<b>volcanic</b>	<b>1361.89</b>	<b>1265.1</b>
isotopic	1491	1391
isotopic	1543	1440
isotopic	1566	1457
isotopic	1734	1657
isotopic	1808	1751
<b>volcanic</b>	<b>1849.55</b>	<b>1796.3</b>
isotopic	1939	1888
isotopic	1953	1904
isotopic	1980	1933
isotopic	2001	1953

isotopic	2026	1980
isotopic	2066	2025
isotopic	2084	2045
<b>volcanic</b>	<b>2117.75</b>	<b>2086.6</b>
isotopic	2138	2107
<b>volcanic</b>	<b>2170.18</b>	<b>2150.9</b>
isotopic	2191	2177
isotopic	2226	2223
isotopic	2236	2235
isotopic	2278	2290
isotopic	2299	2322
isotopic	2333	2370
isotopic	2388	2442
isotopic	2401.5	2459
isotopic	2411	2470
isotopic	2420.5	2483
isotopic	2446.5	2513
isotopic	2485	2565
isotopic	2500	2592

### Table S3

Tie points between the DF and EDC99 ice cores. Volcanic (labelled 'volcanic') tie points are from (38), ice isotopic (labelled 'isotopic') tie points are from this study.

Type	VK depth (m)	EDC99 depth (m)
surface	0	0
isotopic	262	360
isotopic	287	385
isotopic	311	418
isotopic	357	472
isotopic	449	587
isotopic	467	605
isotopic	490	623
isotopic	499	636
isotopic	514	650
isotopic	540	670
isotopic	570	700
isotopic	596	729
isotopic	608	740
isotopic	625	759
isotopic	664	800
isotopic	773	878
isotopic	800	899
isotopic	920	996
isotopic	981	1040
isotopic	1010	1061
isotopic	1062	1101
isotopic	1192	1200
isotopic	1256	1245
isotopic	1450	1412
isotopic	1484	1440
isotopic	1783	1657
<b>Volcanic</b>	<b>1991.93</b>	<b>1804</b>
isotopic	2148	1888
isotopic	2177	1904
isotopic	2235	1933

isotopic	2275	1953
isotopic	2325	1980
isotopic	2402	2025
isotopic	2431	2045
<b>Volcanic</b>	<b>2501.9</b>	<b>2086.6</b>
isotopic	2531	2106
<b>Volcanic</b>	<b>2586.2</b>	<b>2150.9</b>
isotopic	2625	2177
isotopic	2679	2223
isotopic	2693	2235
isotopic	2760	2295
isotopic	2790	2322
isotopic	2827	2353
isotopic	2845	2368
isotopic	2900	2412
isotopic	2937	2442
isotopic	2962	2459
isotopic	2979.5	2470
isotopic	2998	2484
isotopic	3037	2513
isotopic	3102	2566
isotopic	3146	2602
isotopic	3215	2658
isotopic	3230	2674.5
isotopic	3241	2684
isotopic	3310	2750

**Table S4**

Tie points between the Vostok and EDC99 ice cores. Volcanic tie points are from (38). Vostok depth as defined in (31).

Type	TALDICE depth (m)	EDC99 depth (m)
isotopic	1160	800
isotopic	1220	880
isotopic	1256.5	942
isotopic	1282.5	997
isotopic	1303	1060
isotopic	1312	1100
isotopic	1332	1200
isotopic	1365	1390
isotopic	1374.5	1442
isotopic	1404	1658
isotopic	1440	1855
isotopic	1446	1889
isotopic	1463	1906
isotopic	1471	1935
isotopic	1477.5	1952.5
isotopic	1485	1981
isotopic	1493.7	2027
isotopic	1497	2048
isotopic	1508	2093
isotopic	1522.5	2170
isotopic	1528	2222
isotopic	1534	2235
isotopic	1545	2295
isotopic	1582	2500

**Table S5**

Isotopic tie points between the TALDICE and EDC99 ice cores.

LR04 age (yr b1950)	EDC99 depth (m)	EDC age (yr b1950)
0	116.609	3000
13050	452.439	16050
81250	1186.32	82300
105750	1444.53	106900
131950	1745.62	132800
198000	2075.97	198150
215400	2179.01	215500
227800	2229.28	227900
243450	2312.96	245600
286150	2442.81	290450
312450	2512.57	315900
335550	2594.45	337900
424600	2780.09	427250
490050	2841.57	488000
512000	2872.71	509750
533600	2905.15	530400
580750	2996.48	581900
622350	3037.96	628100
714000	3119.87	718750
743650	3138.55	740550
795500	3188.68	800150

**Table S6**

Synchronisation of the LR04 stack with EDC isotopic variations on the EDC3 age scale.

$i$	$T_i$ AT (yr)	$\sigma T_i$ AT (yr)	$T_i$ aCO <sub>2</sub> (yr)	$\sigma T_i$ aCO <sub>2</sub> (yr)	$T_i$ rCO <sub>2</sub> (yr)	$\sigma T_i$ rCO <sub>2</sub> (yr)
0	9000		9000		9000	
1	11684	31	11183	50	11199	59
2	12691	30	12747	73	12757	86
3	14688	42	14433	78	14533	112
4	17984	63	17993	59	18064	64
5	22000		22000		22000	

**Table S7**

Reconstructed break points of the 6 points linear fit procedure for AT, aCO<sub>2</sub> and rCO<sub>2</sub>.

## References and Notes

1. F. Parrenin *et al.*, *Clim. Past* **8**, 1239-1255 (2012).
2. G. B. Dreyfus *et al.*, *Quat. Sci. Rev.* **29**, 28-42 (2010).
3. G. Krinner, D. Raynaud, C. Doutriaux and H. Dang, *J. Geophys. Res.* **105**, 2059-2070 (2000).
4. F. Parrenin *et al.*, *Clim. Past* **3**, 485-497 (2007).
5. L. Loulergue *et al.*, *Nature* **453**, 383-386 (2008).
6. A. Svensson *et al.*, *Clim. Past* **4**, 47-57 (2008).
7. T. Blunier *et al.*, *Clim. Past* **3**, 325-330 (2007).
8. B. Stenni *et al.*, *Quat. Sci. Rev.* **29**, 146 - 159 (2010).
9. R. Bintanja, R. S. Van de Wal and J. Oerlemans, *Nature* **437**, 125-128 (2005).
10. L. E. Lisiecki and M. E. Raymo, *Paleoceanography* **20**, PA1003 (2005).
11. J. Jouzel and L. Merlivat, *J. Geophys. Res.* **89**, 11749-11757 (1984).
12. A. Tarantola, , Elsevier Sci., New York (1987).
13. N. Metropolis, A. Rosenbluth, M. Rosenbluth, A. Teller and E. Teller, *J. Chem. Phys.* **21**, 1087-1092 (1953).
14. W. Hastings, *Biometrika* **57**, 97-109 (1970).
15. F. Parrenin *et al.*, *Clim. Past* **3**, 243-259 (2007).
16. J. Jouzel *et al.*, *Science* **317**, 793-796 (2007).
17. V. Masson-Delmotte *et al.*, *Quat. Sci. Rev.* **29**, 113 - 128 (2010).
18. V. Masson-Delmotte *et al.*, *Clim. Past* **7**, 397-423 (2011).
19. L. C. Sime, E. W. Wolff, K. I. C. Oliver and J. C. Tindall, *Nature* **462**, 342-345 (2009).
20. T. Laepple, M. Werner and G. Lohmann, *Nature* **471**, 91-94 (2011).
21. F. Vimeux, V. Masson, J. Jouzel, M. Stievenard and J. R. Petit, *Nature* **398**, 410-413 (1999).
22. B. Stenni *et al.*, *Science* **293**, 2074-2077 (2001).
23. K. Kawamura *et al.*, *Nature* **448**, 912-917 (2007).
24. R. Uemura *et al.*, *Clim. Past* **8**, 1109-1125 (2012).
25. R. Winkler *et al.*, *Clim. Past* **8**, 1-16 (2012).
26. M. Siddall, G. A. Milne and V. Masson-Delmotte, *Earth Planet. Sci. Let.* **315-316**, 12 - 23 (2012).
27. V. Morgan *et al.*, *Science* **297**, 1862-1864 (2002).
28. A. Landais *et al.*, *Quat. Sci. Rev.* **25**, 49-62 (2006).
29. J. B. Pedro *et al.*, *Clim. Past* **7**, 671-683 (2011).
30. J. B. Pedro, S. O. Rasmussen and T. D. van Ommen, *Clim. Past* **8**, 1213-1221 (2012).
31. J. R. Petit *et al.*, *Nature* **399**, 429-436 (1999).
32. N. Caillon *et al.*, *Science* **299**, 1728-1731 (2003).
33. EPICA community members, *Nature* **429**, 623-628 (2004).

34. O. Watanabe *et al.*, *Nature* **422**, 509-512 (2003).
35. B. Stenni *et al.*, *Nature Geosci* **4**, 46-49 (2011).
36. null EPICA community members, *Nature* **444**, 195-198 (2006).
37. U. Ruth *et al.*, *Clim. Past* **3**, 475-484 (2007).
38. B. Narcisi, J. R. Petit, B. Delmonte, I. Basile-Doelsch and V. Maggi, *Earth Planet. Sci. Let.* **239**, 253-265 (2005).